A COMPARISON OF THEORETICAL AND EXPERIMENTAL PRESSURE DISTRIBUTIONS AT HIGH SPEED ABOUT THE N.A.C.A. 4412 AIRFOIL

Thesis by

Lt. Frank N. Moyers, Air Corps, U. S. A.

In Partial Fulfillment of the Requirements for the Degree of Master of Science in Aeronautical Engineering

California Institute of Technology

Pasadena, California

1940

ACKNOWLEDGEMENTS

The author wishes to express his appreciation to Dr. Th. von Karman for his suggestion of the subject of the present investigation and for helpful criticism during the course of the work.

Thanks are expressed to Dr. W. R. Sears and Dr. Hsue - Shen Tsien for advice and guidance during the investigation.

TABLE OF CONTENTS

NOTATION

$\bar{q}$	Vector velocity
ρ	Density
ρ_0	Density at stagnation point
ρ_1	Free stream density
P_1	Free stream static pressure
p	Static pressure
ϕ	Velocity Potential
w	Velocity in compressible fluid
w_1	Free stream velocity in compressible fluid
W	Velocity in incompressible fluid
W_1	Free stream velocity in incompressible fluid
P	Pressure coefficient for compressible fluid
P_0	Pressure coefficient for incompressible fluid
M	Mach's Number
M_c	Critical Mach's Number
γ	Ratio of specific heats — c_p/c_v = 1.405 for air.
r	Radius vector in the complex plane
θ	Angle in the complex plane
z	Complex coordinate
ζ	Complex coordinate
Γ	Circulation

C_L	Lift Coefficient
C	Chord of airfoil
b	Half distance between singular points in complex plane
v	Velocity in complex plane
ϑ	Angle from wind axis in the complex ζ plane

INTRODUCTION

The general problem of aerodynamics is the determination of the forces and moments imposed on a stationary body immersed in a moving fluid. The problem is soluble if a mathematical calculation of the velocity distribution throughout the fluid can be made. The application of certain restrictions facilitates the calculation. Without great loss of usefulness we may restrict the motion to a steady, uniform, and rectilinear flow from infinity. With considerable loss of usefulness but with tremendous simplification in calculation we may add the further restrictions that the fluid be non-viscous and incompressible. Upon these assumptions the problem may be solved by utilizing two physical relationships, namely, the equations of motion and continuity. Expressed in vector notation these equations are:

(1) $\bar{q} \cdot \nabla \bar{q} = -\frac{\nabla p}{\rho}$ Equation of Motion

(2) $\nabla \cdot \rho \bar{q} = 0$ Equation of Continuity.

Since we have assumed an incompressible fluid, ρ is constant and may be eliminated from equation (2). Thus (2) reduces to an equation for velocity only. We can solve it for velocity, substitute in (1) and obtain the pressure. Knowledge of the pressure distribution enables us to calculate forces and moments.

Unfortunately for a fluid of variable density, i.e. a compressible fluid, we do not obtain a seperation of variables. However we have an additional physical relationship, the equation of state. Expressed mathematically the equation of state is:

(3) $p = p(\rho)$ Equation of State.

Using equations (1), (2), and (3) to eliminate p and ρ we can obtain an equation involving $\bar{q}$ only. The equation will be non-linear and difficult of solution. Tschapligin[1] has shown that the equation can be linearized in two dimensions by using the magnitude of the velocity and its inclination to a chosen axis as independent variables. By this method Tschapligin obtained a general solution in the hodograph plane, but there is difficulty in adapting it to the boundary conditions of practically important physical problems.

As a result of the difficulties in obtaining an exact solution of the equation there have been many attempts to obtain approximate solutions. Probably the most widely used approximation is that given by Glauert[2] and Prandtl. By neglecting the disturbance velocities in comparison with the free-stream velocity they were able to obtain a linear differential equation for the velocity potential:

$$(4) \quad \left(1 - \frac{W_1^2}{a_1^2}\right)\frac{\partial^2\phi}{\partial x^2} + \frac{\partial^2\phi}{\partial y^2} + \frac{\partial^2\phi}{\partial z^2} = 0$$

This equation leads to the conclusion that the pressure coefficient in a compressible fluid is equal to the pressure coefficient at the corresponding point of an incompressible fluid divided by $\sqrt{1-\left(\frac{W_1^2}{a_1^2}\right)}$. Due to its simplicity this relationship has been widely used in practical applications. However the assumptions made by Glauert hold for very slender bodies only, and even then not in the vicinity of stagnation points. Hence a better approximation is desirable.

A method of successive approximations using the exact equation was developed by Janzen[3] and Raleigh.[4] The method is tedious and the convergence very slow if the local velocity of sound is approached. A mechanical method to carry out this process of approximation using an electrical analogy was devised by Taylor,[5] and he obtained fair agreement with some high speed tests made by Stanton. However Taylor's method requires elaborate technique and accurate equipment, and becomes non-convergent as the local velocity of sound is approached.

Demtchenko[6] and Busemann,[7] using Tschapligin's method and approximating linearly to the adiabatic pressure density curve, using the tangent at the state corresponding to the stagnation point, obtained an approximate solution.

Recently Tsien[8] has extended Demtchenko's and Busemann's theory using the tangent to the adiabatic pressure density curve at the point corresponding to the state of the gas in the undisturbed parallel flow.

The purpose of the present investigation is to test the accuracy of Tsien's approximation by applying it to the potential flow about the 4412 airfoil, and comparing the results with the experimental values determined by Stack[9] in the 24 inch high speed tunnel of the N.A.C.A. Certain comparisons, including Glauert's linearized theory, are also included.

The investigation divides itself into two parts: first the determination of the potential flow about the 4412 airfoil, and second the application of Tsien's correction to this flow

and the resultant comparison with experimental results and Glauert's theory. The potential flow is calculated by the method of Karman[10] and Trefftz. The details of this calculation are given in the Appendix.

APPLICATION OF TSIEN'S CORRECTION

As has been stated in the introduction, Tsien's method is to use Tschapligin's transformation and the linear approximation of the adiabatic pressure density relationship at the point corresponding to the state of the gas in the undisturbed parallel flow. Based upon this approximation Tsien obtained the following relationship between density and velocity:

$$(5) \quad \left[\frac{\rho_0}{\rho}\right]^2 = 1 + \left[\frac{w}{a_0}\right]^2$$

Making use of this relationship Tsien found a point transformation between the hodograph plane for an incompressible fluid and that for a compressible fluid. Another transformation was then found between the hodograph plane of the compressible fluid and the physical plane of the compressible fluid.

The general procedure of using the transformations is to start with the hodograph of incompressible flow about the body being investigated, transform to the hodograph of the compressible flow, thence to the physical plane of the compressible flow. This latter transformation involves a correction factor whose magnitude is dependent on the Mach Number. This correction factor is required due to the fact that the incompressible flow about any given body transforms into the compressible flow about a body of slightly different form. However Karman has found that for comparatively thin profiles this correction to the form of the body may be neglected. Upon this basis the following

relationships between compressible and incompressible flow are derived:

$$(6)\quad \frac{w}{w_1} \doteq \frac{|W|}{W_1}\,\frac{1-\lambda}{1-\lambda\left[|W|/W_1\right]^2} \qquad \text{where} \qquad \lambda = \frac{\left(\frac{w}{a}\right)^2}{\left[1+\sqrt{1-\left(\frac{w}{a}\right)^2}\right]^2}$$

$$(7)\quad P = (1+\lambda)\,\frac{1-\left[|W|/W_1\right]^2}{1-\lambda\left[|W|/W_1\right]^2} .$$

Equation (7) gives the correction to be applied to the pressure coefficient of the incompressible flow obtained by the Karman Trefftz method. Equation (7) may be written in terms of pressure coefficients:

$$(8)\quad P = \frac{1+\lambda}{1-\lambda}\,\frac{P_o}{1+\frac{\lambda P_o}{1-\lambda}}$$

Equation (6) is used later to derive a relationship between the pressure coefficient for incompressible flow and critical Mach Number, the critical Mach Number being defined as that at which the local velocity of sound is attained.

It was found convenient to plot a curve of λ vs. M (Fig. 1) and curves of P vs. P_o for certain specific Mach Numbers (Fig. 2). Using the former curve, λ can be found for any arbitrary Mach Number, and using the latter the relationship between P and P_o can be found by using the curve corresponding to the desired Mach Number.

Corrections to the potential flow are made at three angles of attack, and at medium and high Mach Numbers, these being chosen to correspond to certain high speed experimental

tests reported in N.A.C.A. Report No. 646. Theoretical and experimental pressure distributions about the 4412 airfoil are given in Figures 3 to 11 inclusive. Figures 3, 4, and 5 pertain to an angle of attack of -2° ; Figures 6, 7, and 8 to an angle of attack of $-0^{\circ}15'$; Figures 9, 10, and 11 to an angle of attack of $+1^{\circ}52.5'$

In order to obtain a comparison between experimental values of pressure coefficients and those predicted by Tsien's correction, which would be entirely divorced from any possible discrepancies in the potential flow, curves are plotted giving the calculated maximum negative pressure coefficient vs. Mach number. These curves are obtained by applying Tsien's correction to the experimental pressure coefficient at zero Mach Number, the latter pressure coefficient being obtained by extrapolating curves of maximum negative pressure coefficient vs. Mach Number given in N.A.C.A. Report No. 646. Figures 12 and 13 give these curves for upper and lower surfaces, respectively. Curves of experimental values and curves calculated using the correction given by the Glauert theory are also included.

PREDICTION OF CRITICAL MACH NUMBER

The prediction of critical Mach Number from low speed pressure distribution tests is of great importance. Prior to the development of Tsien's compressibility correction this was usually done by using a curve based upon Glauert's linearized theory. This theory resulted in general in the prediction of a higher critical Mach Number than was shown by experimental high speed tests. For this reason it is considered desirable to develop a curve of critical Mach Number vs. low speed pressure coefficient from Tsien's theory.

Starting with Bernoulli's equation for a compressible fluid:

$$(9)\quad \frac{w^2}{2} + \frac{r}{r-1}\frac{p}{\rho} = \frac{w_1^2}{2} + \frac{r}{r-1}\frac{p_1}{\rho_1}$$

and using the relationship $a^2 = \frac{rp}{\rho}$ we can obtain the following equation:

$$(10)\quad \frac{w^2}{w_1^2} = 1 + \frac{2}{(r-1)M^2} - \frac{2a^2}{(r-1)w_1^2}$$

Now if $w = a$, M will be the critical Mach Number, which we will denote by M_c, and $\frac{w}{w_1}$ will be the critical velocity ratio, which we will denote by $\left[\frac{w}{w_1}\right]_c$.
We may thus express the relationship:

$$(11)\quad \left[\frac{w}{w_1}\right]_c = \left[\frac{r-1}{r+1} + \frac{2}{(r+1)M_c^2}\right]^{\frac{1}{2}}$$

Equation (6) may be put in the form:

$$(12)\quad \frac{w}{w_i} = \frac{[1-P_o]^{\frac{1}{2}}}{1+\frac{\lambda P_o}{1-\lambda}}$$

Equating (11) and (12), a relationship between M_c and P_o is obtained. This relationship may be put in a form suitable for calculation by letting $1 - P_o = x^2$ and

$$\left[\frac{r-1}{r+1} + \frac{2}{(r+1)M_c^2}\right]^{\frac{1}{2}} = A$$

Using this notation and simplifying we obtain a quadratic equation in x:

$$(13)\quad A\lambda x^2 + (1-\lambda)x - A = 0$$

The procedure for the solution of this equation is to assume a value of M, take r for air = 1.405, and calculate A. Find λ for the assumed value of M from Fig 1. Substitution of values of λ and A in (13) permits the solution for x, and hence for P_o. The values calculated are:

M	P_o
.35	-3.678
.40	-2.659
.50	-1.465
.60	-0.823
.70	-0.445
.80	-0.211
.90	-0.067
1.0	0.0

The curve is plotted in Fig. 14. Also plotted are the curve based on Glauert's theory, and experimental points for various profiles.

DISCUSSION

The agreement between the calculated and experimental pressure distributions given in Figures 3 to 11 is in some respects very good and in other respects not very good. The general agreement on the upper surface is quite satisfactory, although there is an indication that Tsien's correction underestimates slightly the maximum negative pressure. However this discrepancy is not borne out on the M_c vs. $P_{o_{max}}$ curve, and may be due to variations between the theoretical and experimental low speed flows. The theoretical pressure distributions have been checked against experimental pressure at low Mach Numbers given in N.A.C.A. Report No. 646. The agreement appeared to be excellent, but great accuracy in comparison could not be obtained due to the small scale of the figures in the Report. The comparisons in Figures 3 to 11 suffer for the same reason.

One noteworthy feature of the experimental values for the upper surface is that near the leading edge the pressure coefficients do not show much increase with Mach Number, and in some cases show a decrease. This behavior is contradictory to both the Tsien and Glauert theories, each of which predicts an increase in pressure coefficient, whether positive or negative, with increase in Mach Number. Simple reasoning from the variation in density leads to the expectation of the behavior predicted by theory. It appears possible that some undetermined tunnel wall effects may have distorted the experimental results.

On the lower surface the disagreement is very marked

as the Mach Number is increased. The experimental data shows a shift in the pressure coefficient in a negative direction with increase in Mach Number. This shift is approximately constant over the entire chord of the airfoil. This shift is unexplained by theory and contradicts the conclusions of reasoning from simple physical considerations.

Figures 12 and 13 are curves of maximum negative pressure coefficient vs. Mach Number for the upper and lower surfaces respectively. Curves of Tsien's and Glauert's theories are plotted, together with the experimental curve. The aggreement between Tsien's theory and experiment on the upper surface is clearly shown. The disagreement between experiment and both theories on the lower surface is also clearly shown. It would appear logical to expect all the curves to have a horizontal tangent at $M = 0$. The fact that the experimental curve does not have such a tangent introduces doubt as to the validity of the experimental results.

Two sources of possible error in the experimental results may be suggested. The first is blocking effect due to the relative dimensions of the tunnel and model; the tunnel is of 24 inch diameter and the model of 5 inch chord. The second is measurement of velocity and reference pressure base. Inasmuch as the details of the method of measuring these quantities is unknown to the author it is impossible to speculate as to possible sources of error.

Some error in the theoretical results is to be

expected due to the neglect of small variations in the transformed profile. The calculation of the magnitude of this error is very complicated and is beyond the scope of the present investigation. However it is to be expected that the effect of neglecting the small variations in profile would be greatest near the leading edge, since this region is very sensitive to even small changes in profile.

In Fig. 14 the agreement between Tsien's theory and the experimental airfoil points is very good. One of the lower surface points is quite a distance from the curve, but for reasons already stated too much credence is not placed on the experimental values for the lower surface. The agreement between Tsien's theory and the experimental points for circular and elliptic cylinders varies from fair to poor. It is believed that this is largely due to Reynolds Number effect.

It is concluded from the present investigation that Tsien's compressibility correction results in a much closer approximation to reality than Glauert's. The exact determination of the accuracy of the Tsien correction must wait upon comparison with further experimental tests.

APPENDIX

DEVELOPMENT OF THEORETICAL INCOMPRESSIBLE FLOW

The development of the incompressible flow about the 4412 airfoil is made using a method of conformal transformation developed by Karman and Trefftz. The theory of the method is clearly presented in the appropriate reference. Only the actual mechanics of carrying out the transformation will be presented here.

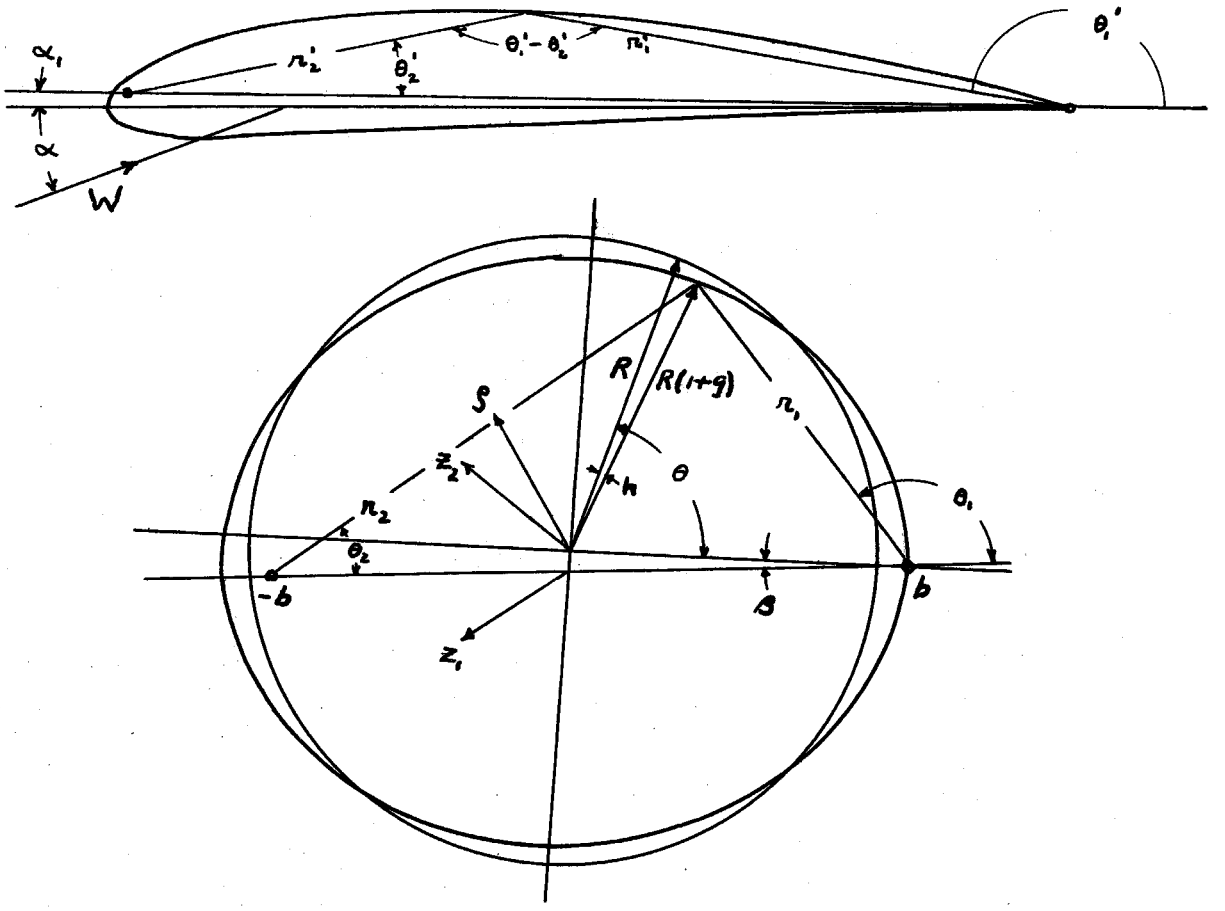

We start with the physical plane containing the airfoil, designated as the z plane. By using the transformation:

$$(14)\qquad \left[\frac{z - Kb}{z + Kb}\right]^{1/K} = \frac{z_1 - b}{z_1 + b}$$

we transform to the z_1 plane. In equation (14) K is determined by the relationship $K = 2 - \frac{\tau}{\pi}$, where τ is the trailing edge angle in radians. For the actual calculation of the transformation it was found convenient to express equation (14) in polar coordinates:

$$(15)\qquad \left[\frac{r_1'}{r_2'}\right]^{1/K} e^{i\left(\frac{\theta_1' - \theta_2'}{K}\right)} = \frac{r_1}{r_2} e^{i(\theta_1 - \theta_2)}$$

The airfoil was then laid out on the z plane to a convenient scale. One singular point was taken at the trailing edge and the other singular point on the least radius of curvature of the leading edge at a point midway between the leading edge and the center of curvature. This method of selection of the forward singular point has been suggested by Theodorsen. The position of the singular points in the z plane having been determined, the radius vectors r_1' and r_2', and the tangents of the angles θ_1' and θ_2' were determined for selected points by physical measurement. The trailing edge angle τ was then calculated and found to be $18.24^\circ = 0.319$ radians. Then from $K = 2 - \frac{\tau}{\pi}$, K was found to be 1.899. Then from (15) were calculated:

$$\frac{r_1}{r_2} = \left[\frac{r_1'}{r_2'}\right]^{1/K} \qquad \theta_1 - \theta_2 = \frac{\theta_1' - \theta_2'}{K}$$

for the points previously selected.

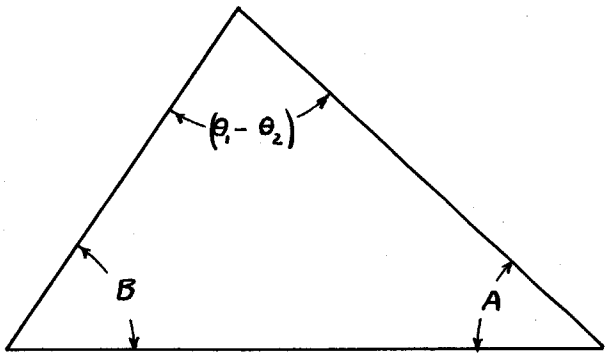

Now in the z_1 plane, for any selected point we have a triangle with the ratio of two sides and the included angle known. We must completely determine the triangle from this knowledge. In the sketch the problem is to calculate the angles A and B. We proceed thus:

Let $\frac{r_1}{r_2} = R$ $\qquad 180^\circ - (\theta_1 - \theta_2) = C$

then $R = \frac{\sin B}{\sin A}$

and $A = C - B$

$\therefore \sin A = \sin(C - B) = \sin C \cos B - \cos C \sin B$

Substituting $\sin A = \frac{\sin B}{R}$ we obtain

$\sin B = R(\sin C \cos B - \cos C \sin B)$

$$\tan B = \frac{R \sin C}{1 + R \cos C}$$

$$\tan A = \tan\left[180^\circ - (\theta_1 - \theta_2) - B\right]$$

Hence A and B are determined.

A convenient base between singular points was next laid off in the z_1 plane and from these singular points A

and B were laid out graphically from their tangents. The intersection of the lines defining A and B determined the point z_1 corresponding to the selected point in the z plane. This process was carried out for several points on the upper and lower surfaces of the airfoil. As may be seen from Fig. 16, the resulting curve in the z_1 plane is approximately circular. The area of this figure was measured using a planimeter and the radius of a circle of equal area calculated. This circle was drawn on a seperate sheet of paper, representing the ζ plane. Then by superposition of the circle sheet on the z_1 plane the position of the center of the circle to give equal areas inside and outside the figure in the z_1 plane was found. The center was then transferred to the z_1 plane and became the origin of coordinates for a z_2 plane. The relation between z_1 and z_2 is given by $z_2 + D = z_1$, where D is a constant complex number, giving the position of the origin in the z_2 plane relative to the origin in the z_1 plane.

Having located the origin in the z_2 plane an orthogonal set of axes was introduced, one axis passing through the origin and the trailing edge singular point. The ζ plane was then superimposed upon the z_2 plane with origins coinciding. In these planes we have two curves, one a true circle and one an approximate circle. We wish to obtain a transformation between these curves. If we let

$$\zeta = z_2\left[1 + f(z_2)\right]$$

$$r = R\left[1 + g(\theta_2)\right]$$

$$\theta_2 = \theta + h(\theta_2)$$

where f, g, and h are small quantities, it has been shown by Karman that if we let

$$\log (1 + f) = \sum_1^{\infty} \frac{(a_n + ib_n)}{\zeta^n} R^n$$

we have

$$g + ih = \sum_1^{\infty} (a_n + ib_n) e^{-in\theta}$$

or

$$g = \sum_1^{\infty} \left[a_n \cos n\theta + b_n \sin n\theta\right]$$

$$h = \sum_1^{\infty} \left[b_n \cos n\theta - a_n \sin n\theta\right]$$

The expression for g is exactly that of a Fourier series. Hence if we measure gR for selected points and expand g as a Fourier Series we may determine the coefficients a_n and b_n. The expansion of g in a Fourier series was carried out by a numerical system and the following expression obtained:

$$(16)\quad g = .00326\cos\theta + .02538\cos 2\theta - .00028\cos 3\theta$$
$$- .00147\cos 4\theta + .00138\cos 5\theta - .00027\cos 6\theta$$
$$- .00135\sin\theta + .00864\sin 2\theta - .00322\sin 3\theta$$
$$+ .00317\sin 4\theta - .00155\sin 5\theta + .00178\sin 6\theta$$

From this we may write:

$$(17)\quad h = -.00135\cos\theta + .00864\cos 2\theta - .00322\cos 3\theta$$
$$+ .00317\cos 4\theta - .00155\cos 5\theta + .00178\cos 6\theta$$
$$- .00326\sin\theta - .02538\sin 2\theta + .00027\sin 3\theta$$
$$+ .00147\sin 4\theta - .00138\sin 5\theta + .00027\sin 6\theta$$

and as later we will need $\frac{dh}{d\theta}$ to obtain a relation between velocities in the z and ζ planes we may differenciate (17), obtaining:

$$(18)\quad \frac{dh}{d\theta} = .00135\sin\theta - .01728\sin 2\theta + .00966\sin 3\theta$$
$$- .01268\sin 4\theta + .00775\sin 5\theta - .01068\sin 6\theta$$
$$- .00326\cos\theta - .05076\cos 2\theta$$
$$+ .00081\cos 3\theta + .00588\cos 4\theta - .00690\cos 5\theta$$
$$+ .00162\cos 6\theta$$

Due to a mistake in the calculations of the coefficients in the Fourier expansion of g, the axis of reference for that expansion makes an angle of 15° clockwise with the axis through the origin and the singular point at the trailing edge. This in no way affects the validity of the series. However, since for succeeding computations it is convenient to measure angles from

the latter axis, in plotting curves of g, h, and $\frac{dh}{d\theta}$ (Fig. 17) the origin was shifted to make the measurement of θ from the axis through the origin and the trailing edge singular point.

The foregoing calculations furnish a means of transforming the 4412 airfoil into a circle in the ζ plane. Our final aim is to find the transformation of velocities between the two planes, since from velocities it is possible to calculate pressure by Bernoulli's equation. The theoretical potential flow about a circular cylinder is known. A transformation of velocity in the ζ plane to velocity in the z plane permits the calculation of pressure distribution in the z plane.

It is known that:

$$|v_z| = |v_\zeta|\left|\frac{d\zeta}{dz}\right| = |v_\zeta|\left|\frac{d\zeta}{dz_2}\right|\left|\frac{dz_2}{dz_1}\right|\left|\frac{dz_1}{dz}\right|$$

Since a transfer of origin only is involved:

$$\left|\frac{dz_2}{dz_1}\right| = 1$$

It may be readily shown that for points on the circle in the ζ plane:

$$\left|\frac{d\zeta}{dz_2}\right| = (1 - q - \frac{dh}{d\theta})$$

and for points on the curve in the z_1 plane:

$$\left|\frac{dz_1}{dz}\right| = \frac{r_1' r_2'}{r_1 r_2}$$

Hence there exists the following relation between the magnitude of the velocities at the surfaces of the airfoil and circle:

(19) $$v_z = v_\zeta \left(1 - \varepsilon - \frac{dh}{d\theta}\right) \frac{r_1' r_2'}{r_1 r_2}$$

Consideration must now be given to v_ζ . We are interested only in the velocity on the surface of the circular cylinder, which is tangent to the cylinder. If we call this velocity v_ϑ , potential flow theory furnishes the relation:

$$v_\vartheta = -2W \sin\vartheta - \frac{\Gamma}{2\pi R}$$

The value of Γ must be determined. This quantity is usually determined by the Kutta - Jowkowski condition, i.e., that the velocity at the trailing edge must not be infinite. However, in a viscous fluid, such as air, the full Kutta - Jowkowski circulation is not generated due to the boundary layer, which effectively changes the shape of the profile. In general, the experimental circulation is found to be approximately 0.9 of the Kutta - Jowkowski circulation. In order to obtain a pressure distribution about the airfoil which will agree with the experimentally measured pressure distribution, it is necessary to determine Γ such that the lift coefficient in the theoretical plane is the same as that observed experimentally at the particular angle of attack under consideration. The experimental lift coefficients, determined in the present case by integration of experimental pressure distributions, for three angles of attack are:

α	C_L
-2°	0.28
$-0^\circ 15'$	0.45
$+1^\circ 52.5'$	0.67

Potential theory gives $L = \rho W \Gamma = \frac{\rho}{2} W^2 C C_L$

and $\Gamma = 2\pi R v_\theta$

These relations give $v_{\theta_r} = \frac{WC}{4\pi R} C_L$

In the present type of transformation $C = 2kb(1 + e)$ and $R = b(1 + u)$, where e and u are small quantities. For the case of the 4412 airfoil it is found that $e = .0077$ and $u = .056$. Substitution for R, C, e, and u in the expression for v_{θ_r} yields: $v_{\theta_r} = 0.289 W C_L$

Hence $v_\theta = -W[2 \sin \theta + 0.289 C_L]$

Substituting in (19) the velocity transformation becomes:

$$(20) \quad v_z = -W[2 \sin \theta + 0.289 C_L]\left[1 - q - \frac{dh}{d\theta}\right]\frac{r_1' r_2'}{r_1 r_2}$$

By using Bernoulli's equation a dimensionless pressure coefficient of the form $(P - P_0)/\frac{\rho}{2} W^2$ may be derived from (20):

$$(21) \quad P = 1 - \left[(2 \sin \theta + 0.289 C_L)\left(1 - q - \frac{dh}{d\theta}\right)\frac{r_1' r_2'}{r_1 r_2}\right]^2$$

To use (21) we go back to our originally selected points on the airfoil and their transformed positions in the z, plane, measure r_1', r_2', r_1, & r_2, and compute the ratio $r_1' r_2'/r_1 r_2$, being

careful to take into account the difference, if any, in the scale of the drawings. Then for each point measure the angle θ_2 in the z_2 plane. From Fig. 17 obtain the corresponding values of g, h, and $\frac{dh}{d\theta}$. Using the relation $\theta = \theta_2 - h$ obtain θ, which is the angle in the ζ plane corresponding to θ_2 in the z_2 plane. This angle is measured from the axis through the origin and the trailing edge singular point. However the angle ψ in the expression for P must be measured from a wind axis through the origin. Hence to obtain ψ from θ it is necessary to subtract α, α_1, and β (see sketch, page 13). The angles α_1 and β are constant and their sum in the case of the 4412 airfoil is 4.7°.

The above data is all that is required for the calculation of pressure coefficients. The calculation is carried out for three angles of attack in this investigation. The results are plotted in Figures 3, 6, and 9.

DISCUSSION

The pressure distribution derived theoretically agrees very well with the experimental curves. However, in the neighborhood of the leading edge the theoretical points show considerable scatter. This scatter is believed to be due to the sensitivity of the method to small errors in measurement of angles in this region. It was found that 0.1° error in ν for points near the leading edge would account for the scatter. Unfortunately there are many opportunities for inaccuracies in the determination of ν. There are three graphical layout and measure operations, in addition to many numerical calculations. Also contributing to errors in ν is the series expansion of h, which does not converge rapidly. The effect of errors in g and $\frac{dh}{d\theta}$ appear much less important in the neighborhood of the leading edge that similar errors in h.

In order to obtain smooth curves for pressure distributions corrected for compressibility, the theoretical incompressible pressure coefficient points were used to construct a faired curve. Points from this curve were corrected for compressibility and compared with experimental results.

The value of Γ used in the determination of theoretical velocity corresponds to an experimental lift coefficient. The value was in all cases less than that determined by the Kutta - Jowkowski condition. As a result an infinite velocity,

and hence an infinite negative pressure, theoretically occurs at the trailing edge. To avoid this condition, and yet keep commensurate with the experimental lift, Pinkerton, in N.A.C.A. Report No. 563, has given a method of deforming the airfoil near the trailing edge to move the trailing edge up to a point where the Kutta - Jowkowski circulation will agree with the experimental lift. However, Betz" has shown that the velocity may be allowed to become infinite at the trailing edge without affecting the pressure distribution except in the immediate proximity. Betz' procedure was followed in this investigation and excellent agreement with experiment was obtained as far back as 0.9C, which was the farthest aft point calculated. The pressure distribution over the front 0.9C is believed to be of the greatest interest for the application of Tsien's correction, and comparison with experiment.

REFERENCES

1 Tschapligin, A., Ueber Gasstrahlen, Wissensch. Annalen d. Univ. Moskau, Phys. - Math. Kl., vol. 21 (1904), page 1.

2 Glauert,H., The Effect of Compressibility on the Lift of an Airfoil, RM 1135, British A.R.C., 1928.

3 Janzen, O., Beitrag zu einer Theorie der Stationaren Stromung Kompressibler Flussigkeiten., Phys. Zeitschr. vol. 14 (1913), page 639.

4 Lord Rayleigh, On the Flow of Compressible Fluid past an Obstacle., Phil. Mag., vol. 32 (1916), page 1. Scientif Pap., vol. 6, page 402.

5 Taylor, G.I., A mechanical Method for Solving Problems of Flow in Compressible Fluids., R.M. 1195, British A.R.C.

6 Demtchenko, B., Sur les Mouvements lents des Fluides Compressibles, Comptes Rendus, vol. 194 (1932), page 1218. Variation de la Resistance aux Faibles Vitesses sous l'Influence de la Compressibilite, Comptes Rendus, vol. 194 (1932), page 1720.

7 Busemann, A., Die Expansionberichtigung der Kontraktionsziffer von Blenken., Forschung, vol. 4 (1933), pages 186 - 187. Hodengraphenmethode der Gasdynamik, Z.A.M.M., vol. 12 (1937), pages 73 - 79.

8 Tsien, H., Two Dimensional Subsonic Flow of Compressible Fluids, Journal of Aero. Sci., vol. 6, No. 10, August 1939.

9 Stack, J., The Compressibility Burble and the Effect of Compressibility on Pressures and Forces Acting on an Airfoil. N.A.C.A. Report No. 646.

10 V. Karman, Th., Durand's Aerodynamic Theory, vol. 2, Chap. 2, Secs. 21, 24.

11 Betz, A., Durand's Aerodynamic Theory, vol. 4, page 18.

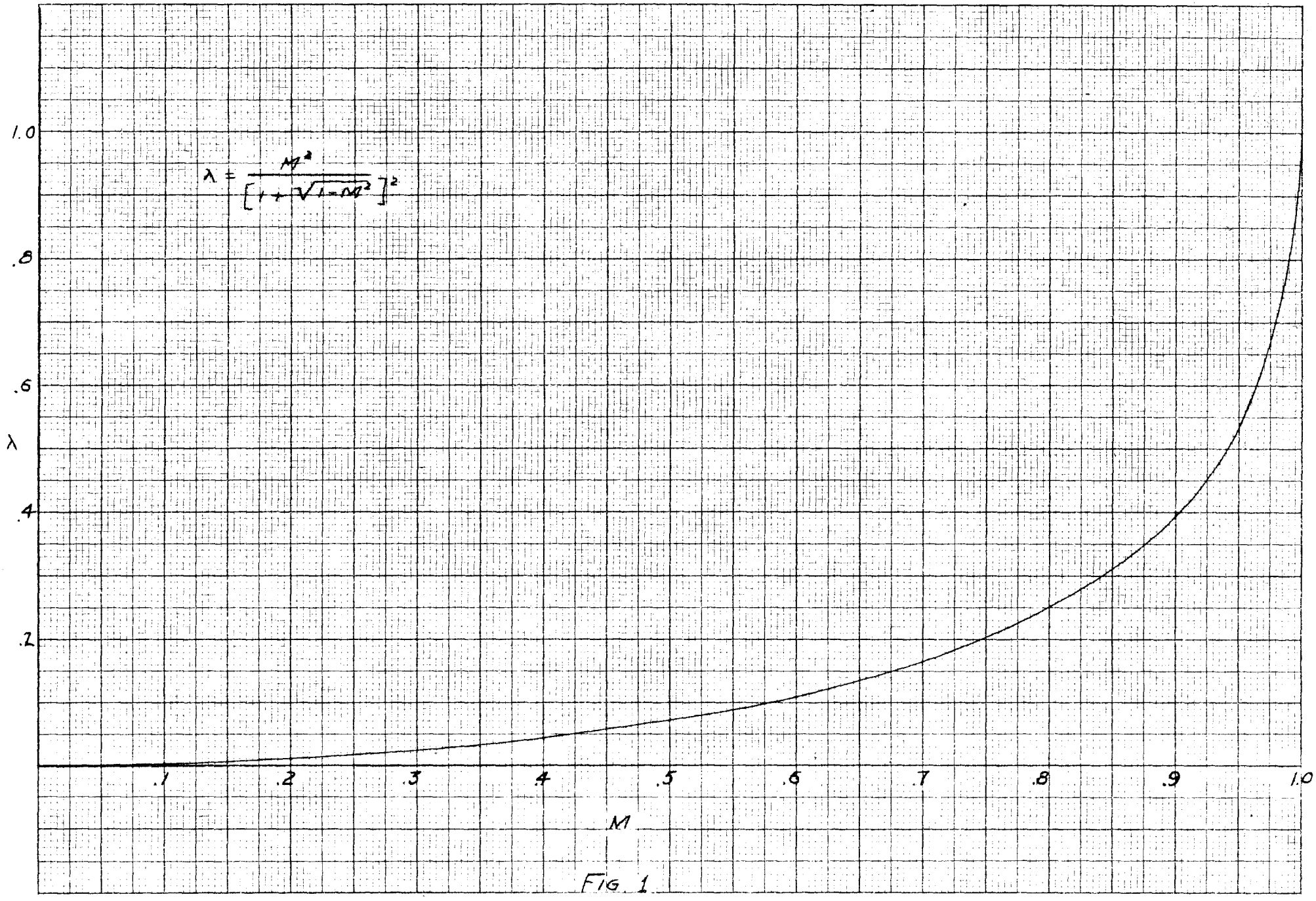

FIG. 1

PRESSURE COEFFICIENT OF COMPRESSIBLE FLUID VS.
PRESSURE COEFFICIENT OF INCOMPRESSIBLE FLUID

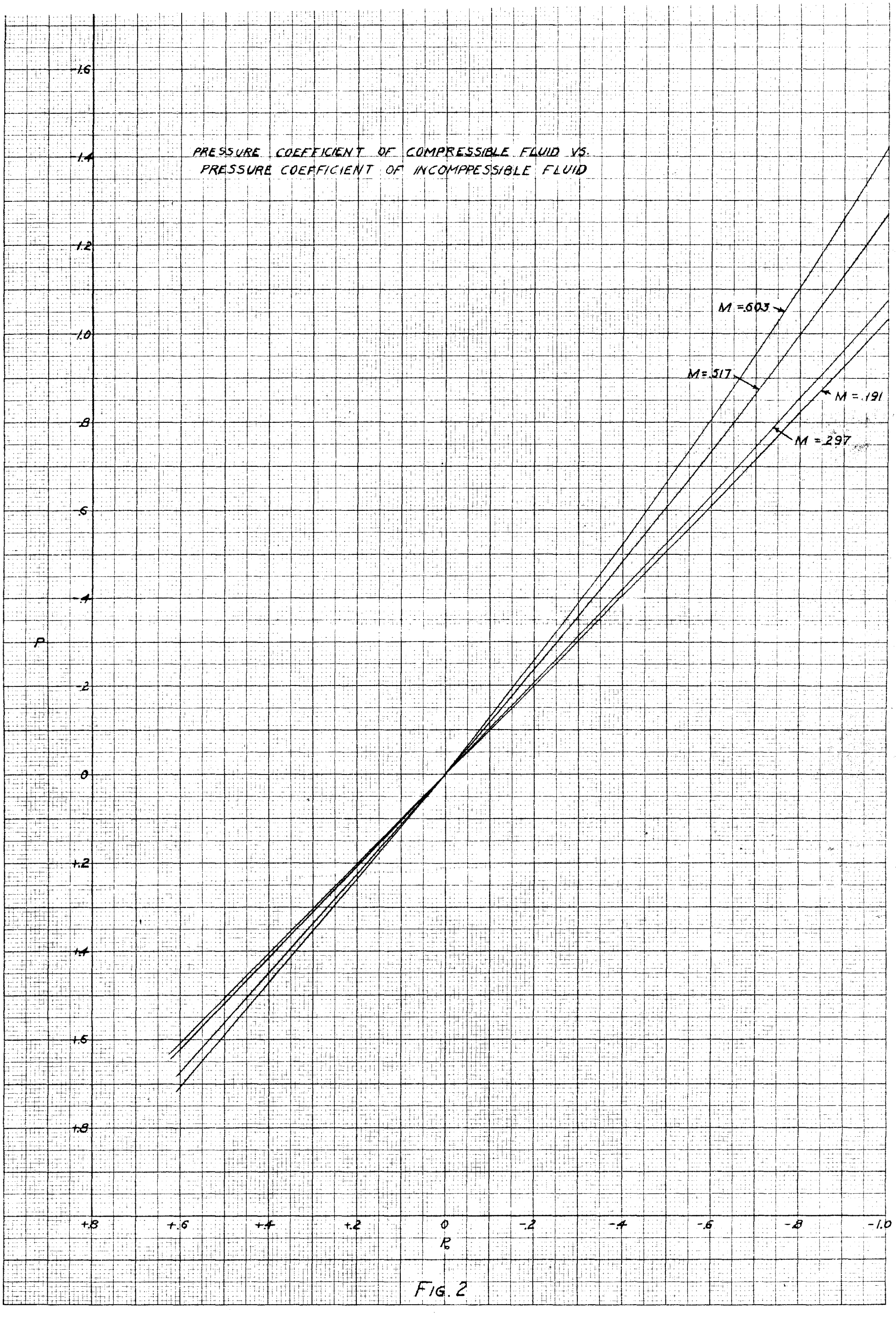

FIG. 2

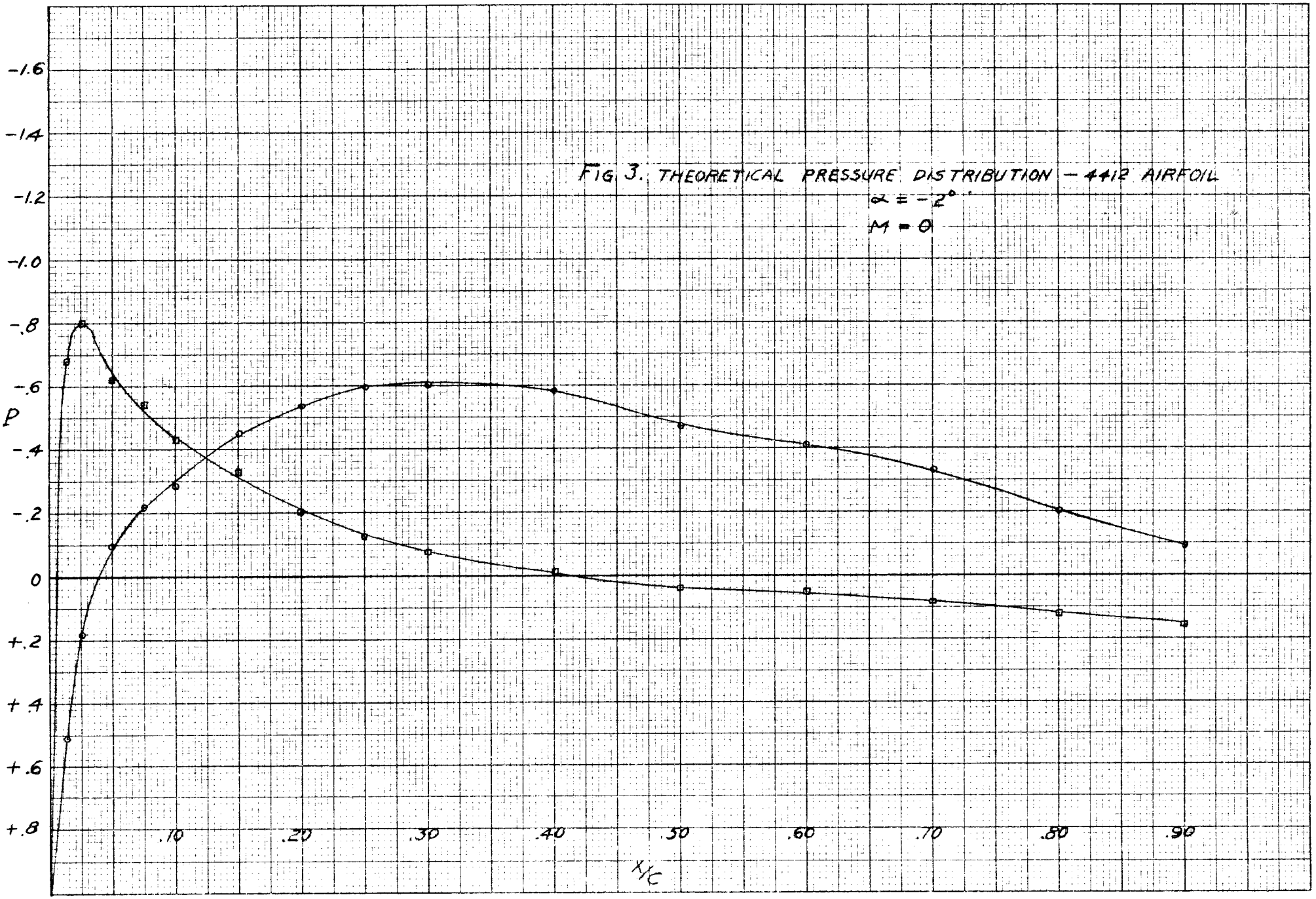

FIG 3. THEORETICAL PRESSURE DISTRIBUTION — 4412 AIRFOIL

$\alpha = -2°$

$M = 0$

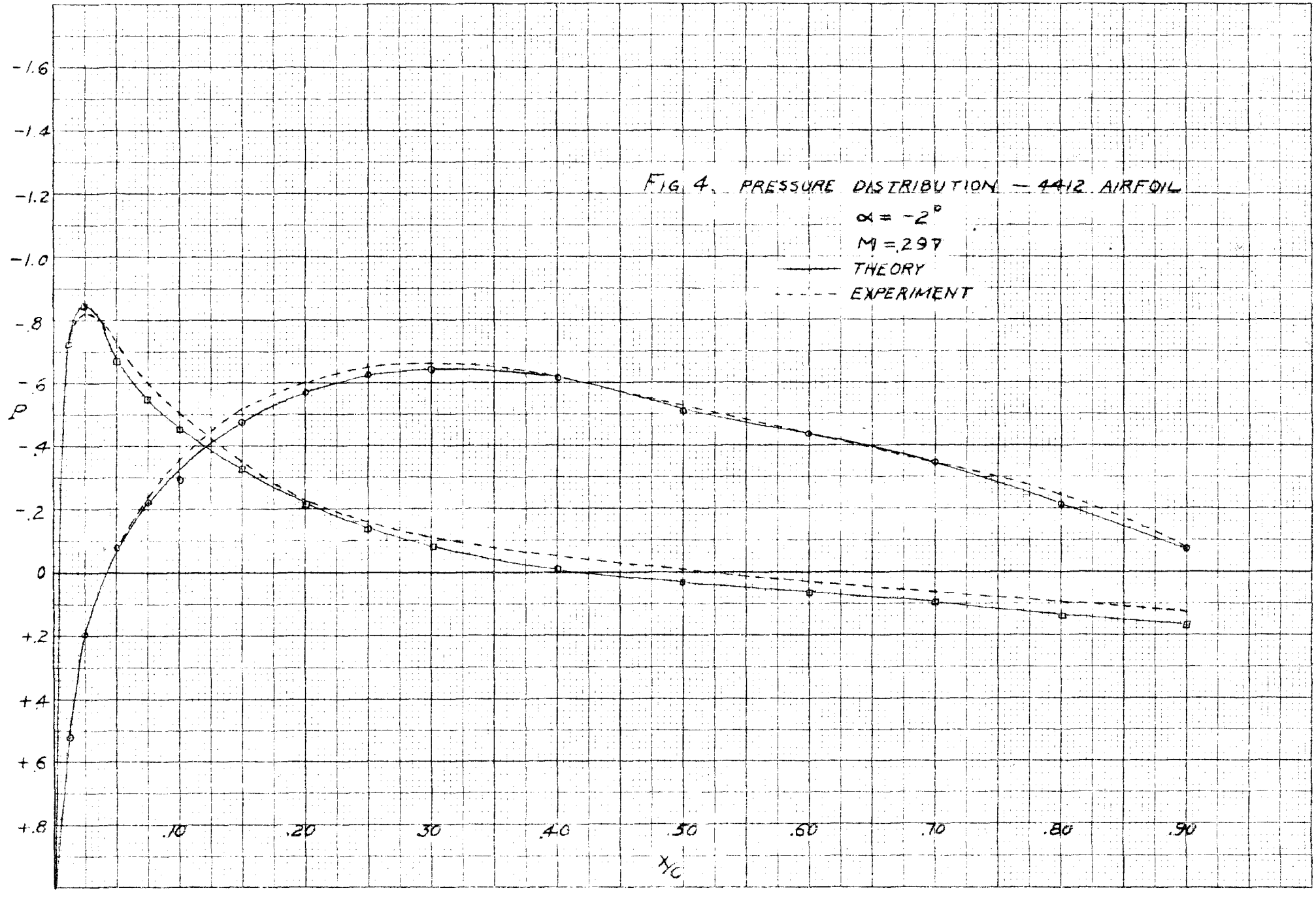
FIG. 4. PRESSURE DISTRIBUTION — 4412 AIRFOIL
α = -2°
M = .297
THEORY
EXPERIMENT
-1.6
-1.4
-1.2
-1.0
-.8
-.6
-.4
-.2
0
+.2
+.4
+.6
+.8
P
.10
.20
.30
.40
.50
.60
.70
.80
.90
X/C

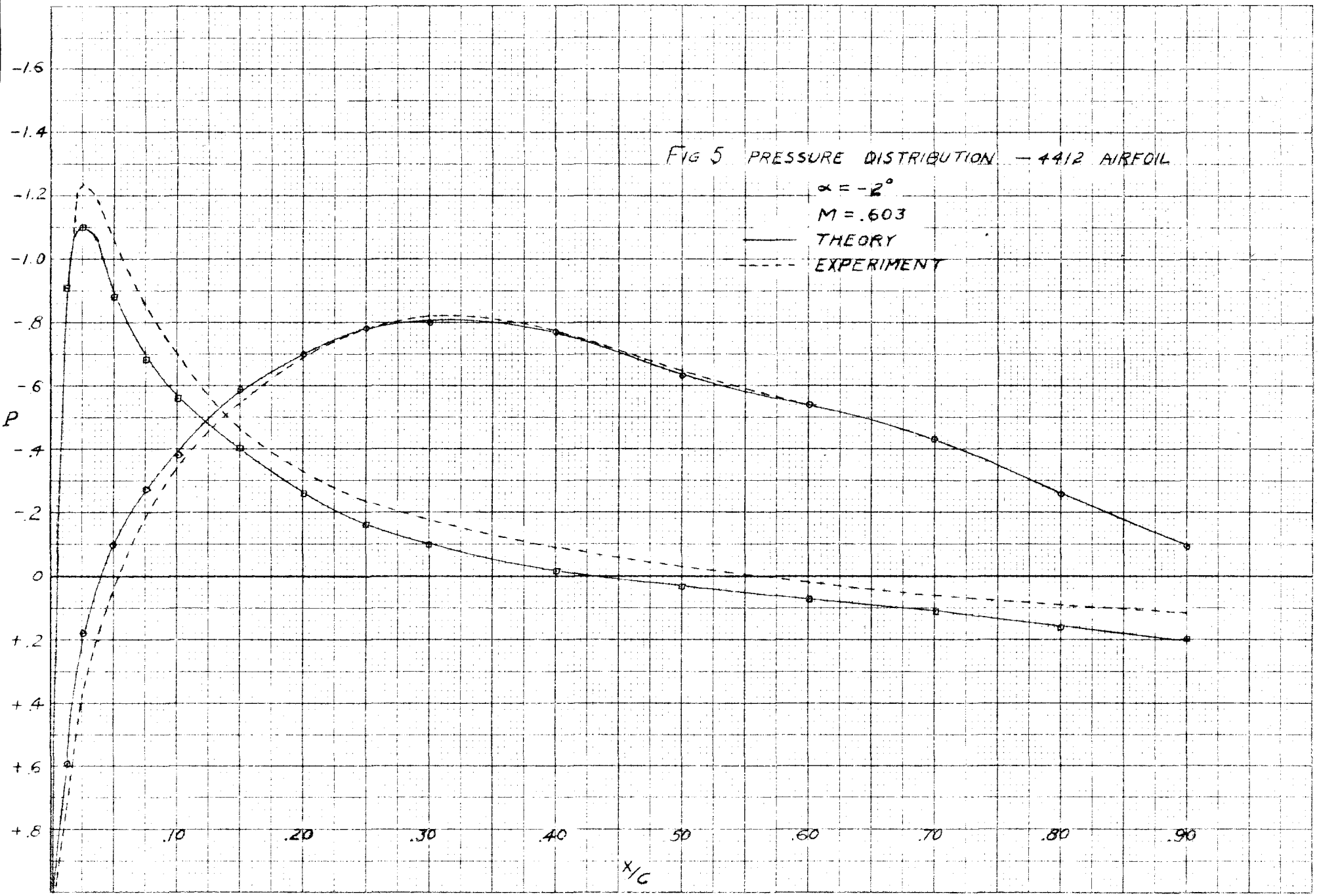
FIG 5 PRESSURE DISTRIBUTION — 4412 AIRFOIL
α = -2°
M = .603
THEORY
EXPERIMENT
-1.6
-1.4
-1.2
-1.0
-.8
-.6
-.4
-.2
0
+.2
+.4
+.6
+.8
P
.10
.20
.30
.40
.50
.60
.70
.80
.90
X/C

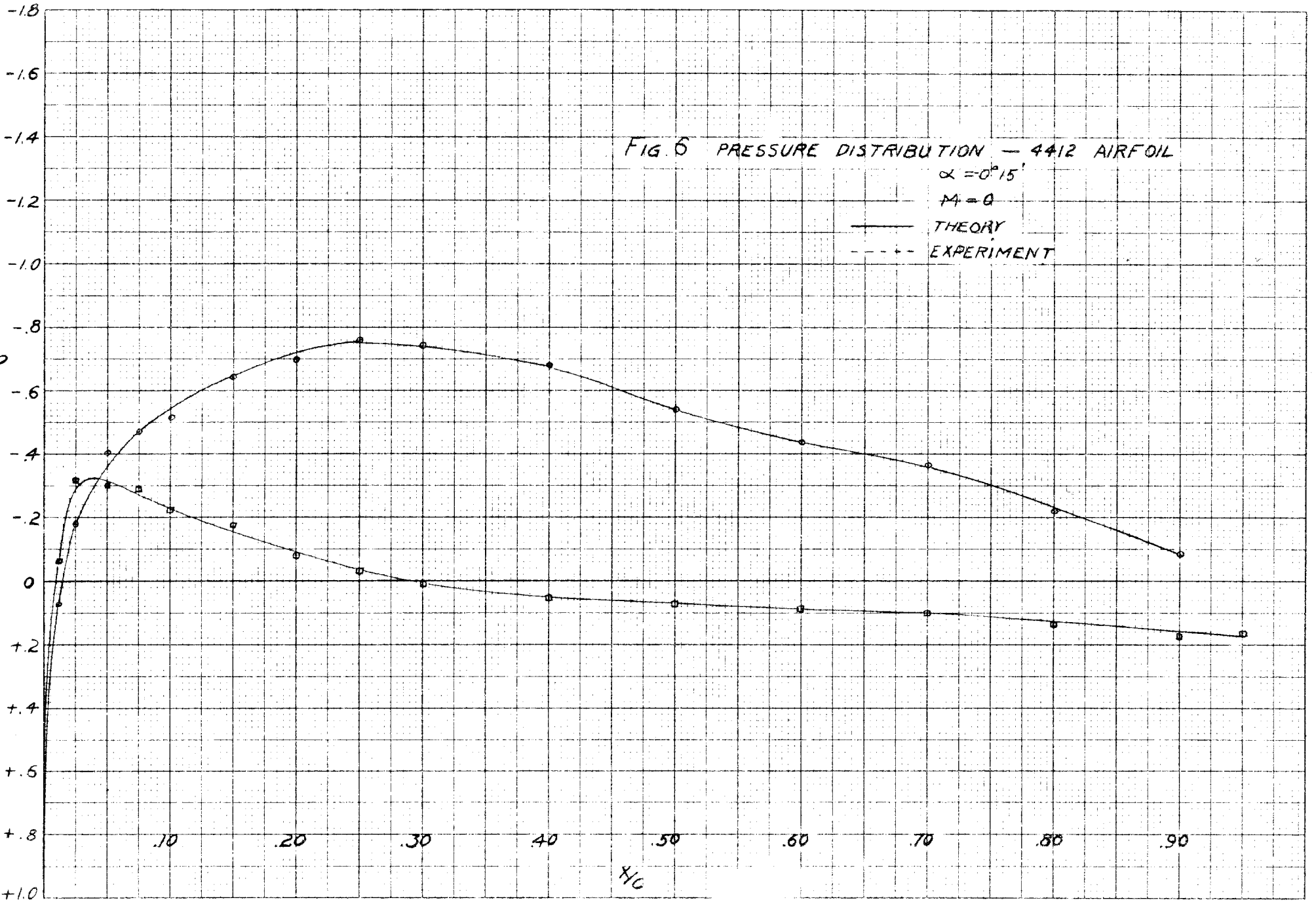
FIG. 6 PRESSURE DISTRIBUTION — 4412 AIRFOIL
α = -0°15'
M = 0
THEORY
EXPERIMENT
-1.8
-1.6
-1.4
-1.2
-1.0
-.8
-.6
-.4
-.2
0
+.2
+.4
+.6
+.8
+1.0
.10
.20
.30
.40
.50
.60
.70
.80
.90
X/C

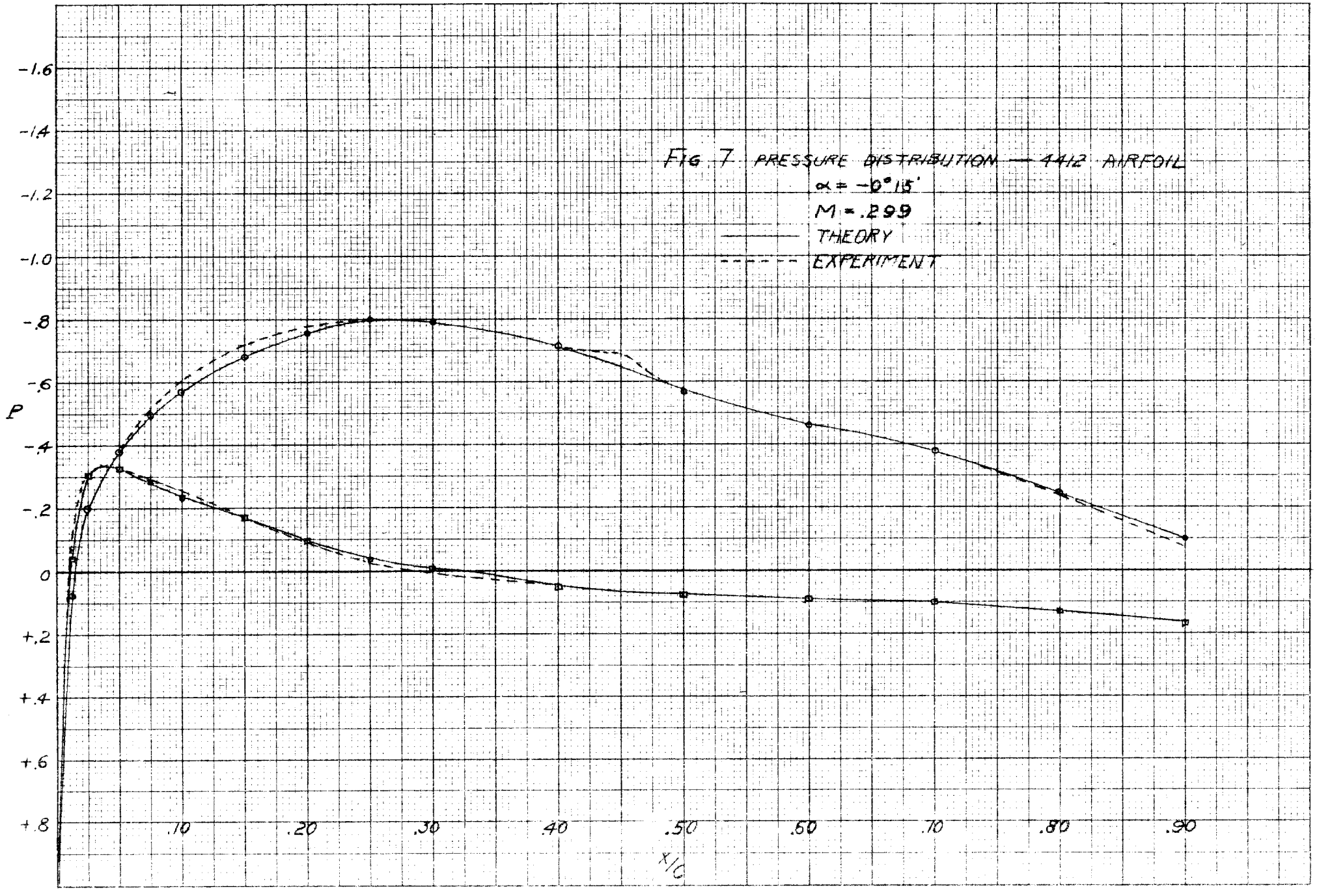
FIG 7 PRESSURE DISTRIBUTION — 4412 AIRFOIL
α = -0°15'
M = .299
THEORY
EXPERIMENT
-1.6
-1.4
-1.2
-1.0
-.8
-.6
-.4
-.2
0
+.2
+.4
+.6
+.8
P
.10
.20
.30
.40
.50
.60
.70
.80
.90
X/C

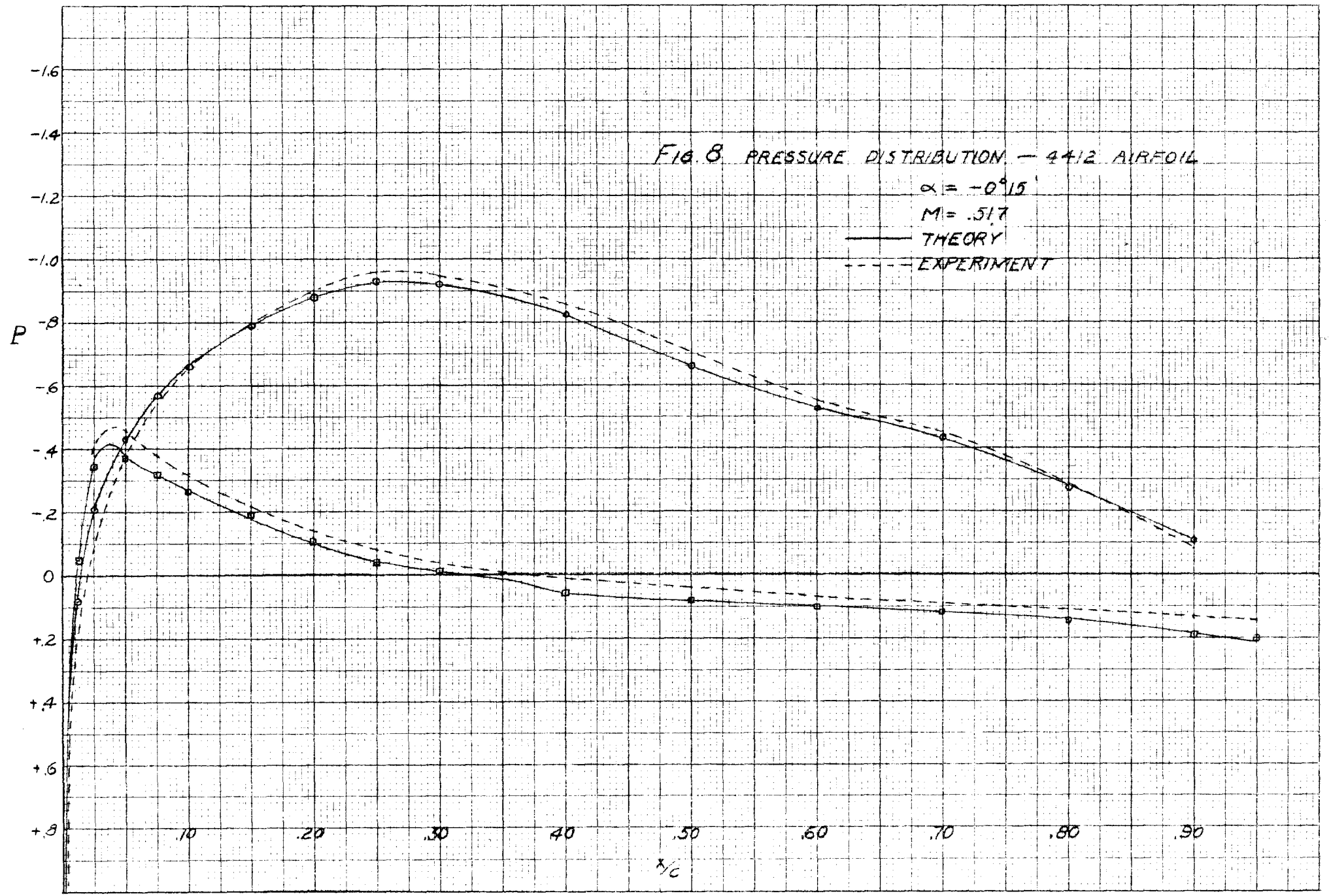
FIG. 8 PRESSURE DISTRIBUTION — 4412 AIRFOIL
α = −0°15'
M = .517
THEORY
EXPERIMENT
P
−1.6
−1.4
−1.2
−1.0
−.8
−.6
−.4
−.2
0
+.2
+.4
+.6
+.8
.10
.20
.30
.40
.50
.60
.70
.80
.90
x/c

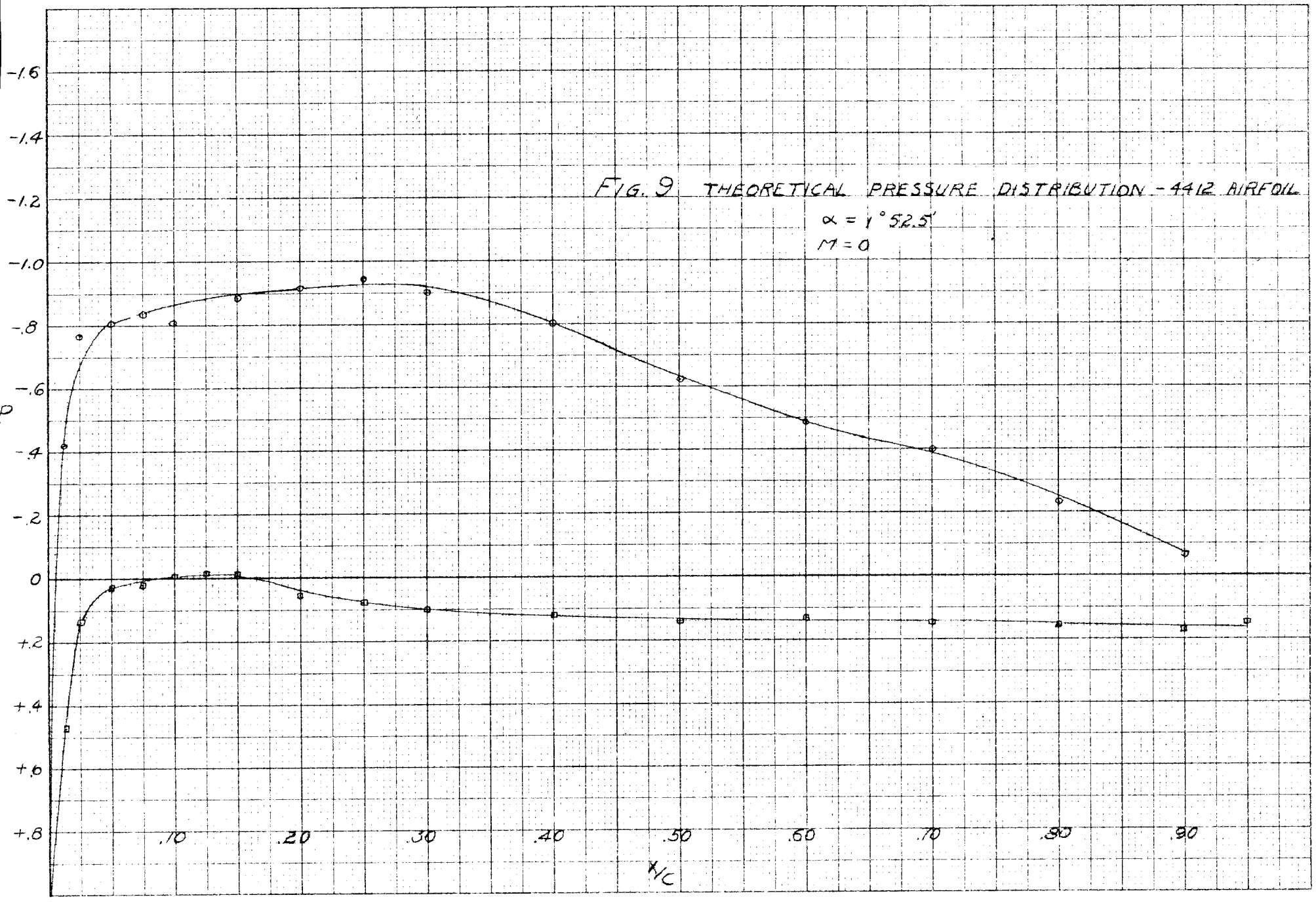

FIG. 9 THEORETICAL PRESSURE DISTRIBUTION - 4412 AIRFOIL

$\alpha = 1^\circ 52.5'$

$M = 0$

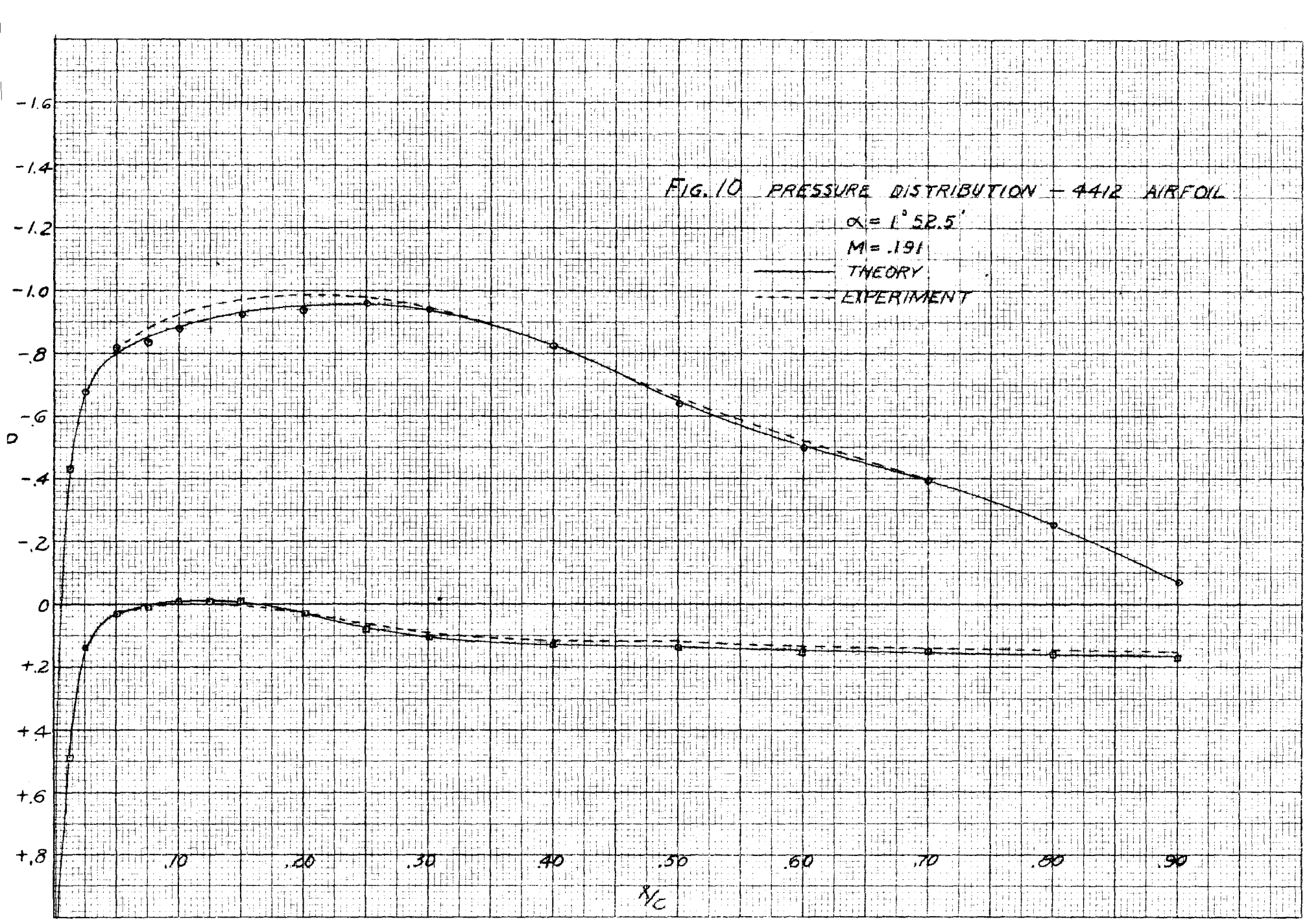
FIG. 10 PRESSURE DISTRIBUTION — 4412 AIRFOIL
α = 1° 52.5'
M = .191
THEORY
EXPERIMENT
-1.6
-1.4
-1.2
-1.0
-.8
-.6
-.4
-.2
0
+.2
+.4
+.6
+.8
Cp
.10
.20
.30
.40
.50
.60
.70
.80
.90
x/c

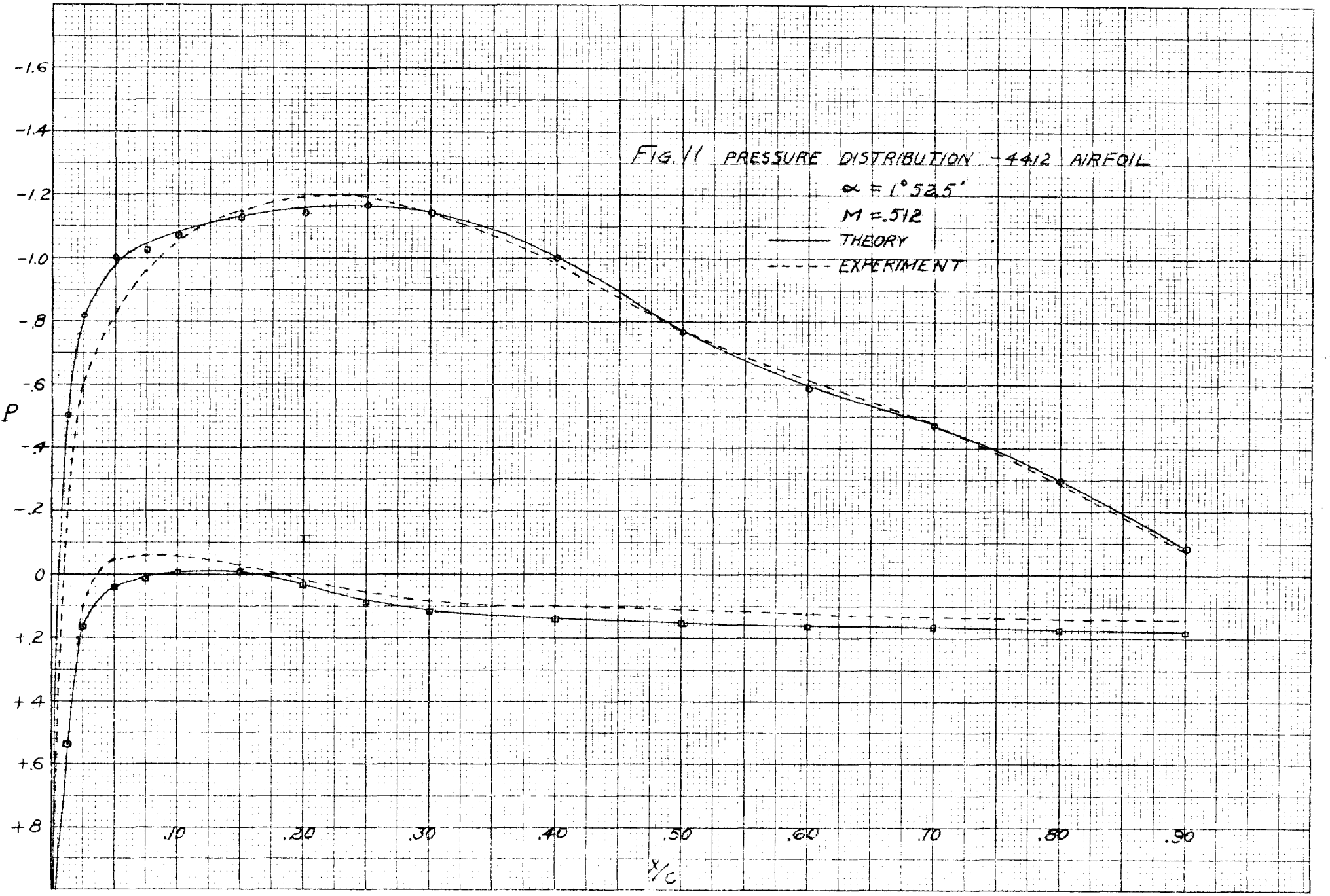
FIG. 11 PRESSURE DISTRIBUTION -4412 AIRFOIL
α = 1° 52.5'
M = .512
THEORY
EXPERIMENT
-1.6
-1.4
-1.2
-1.0
-.8
-.6
-.4
-.2
0
+.2
+.4
+.6
+.8
P
.10
.20
.30
.40
.50
.60
.70
.80
.90
X/C

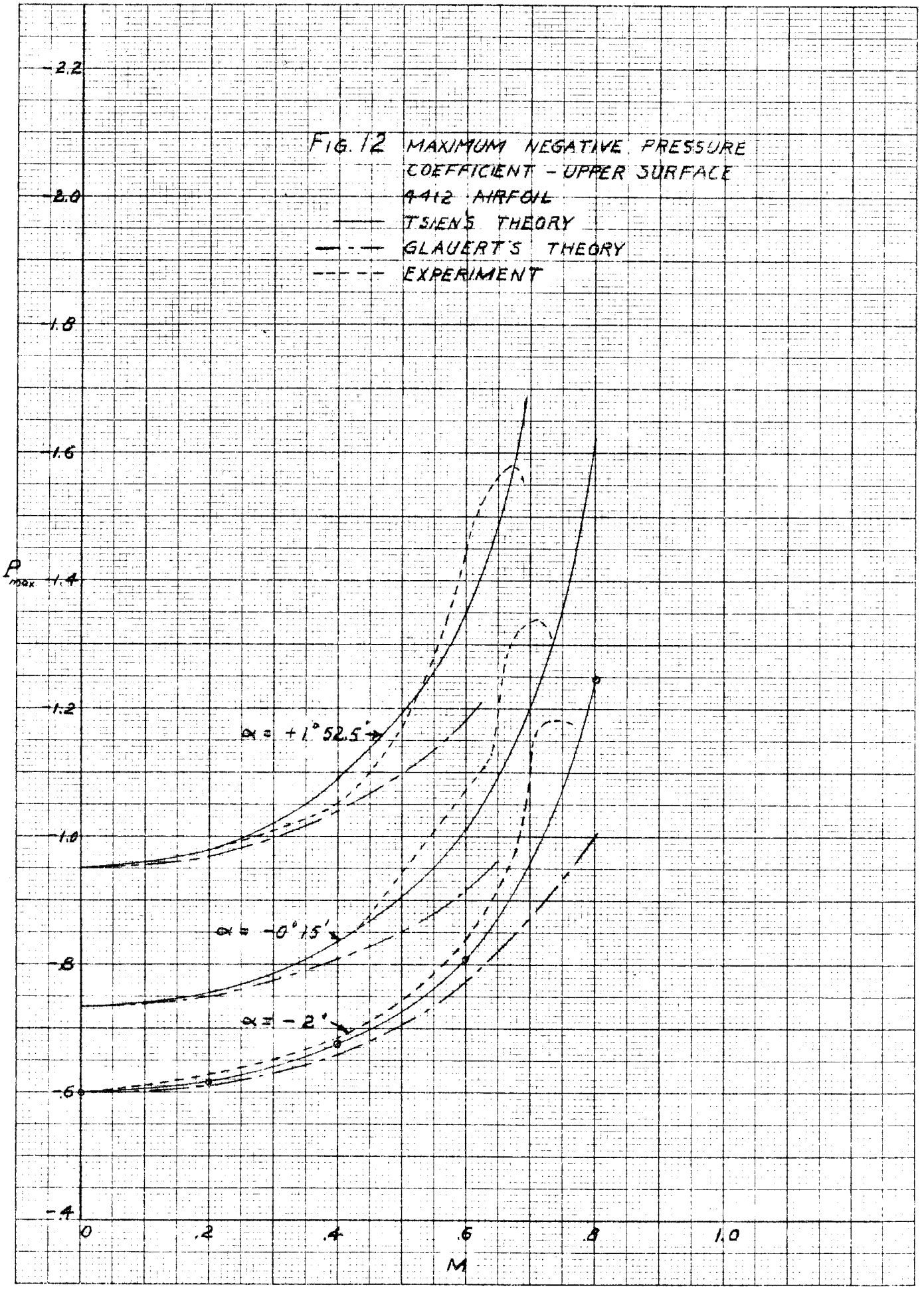
FIG. 12 MAXIMUM NEGATIVE PRESSURE COEFFICIENT - UPPER SURFACE
4412 AIRFOIL
TSIEN'S THEORY
GLAUERT'S THEORY
EXPERIMENT
P_{max}
-2.2
-2.0
-1.8
-1.6
-1.4
-1.2
-1.0
-.8
-.6
-.4
α = +1°52.5'
α = -0°15'
α = -2°
0
.2
.4
.6
.8
1.0
M

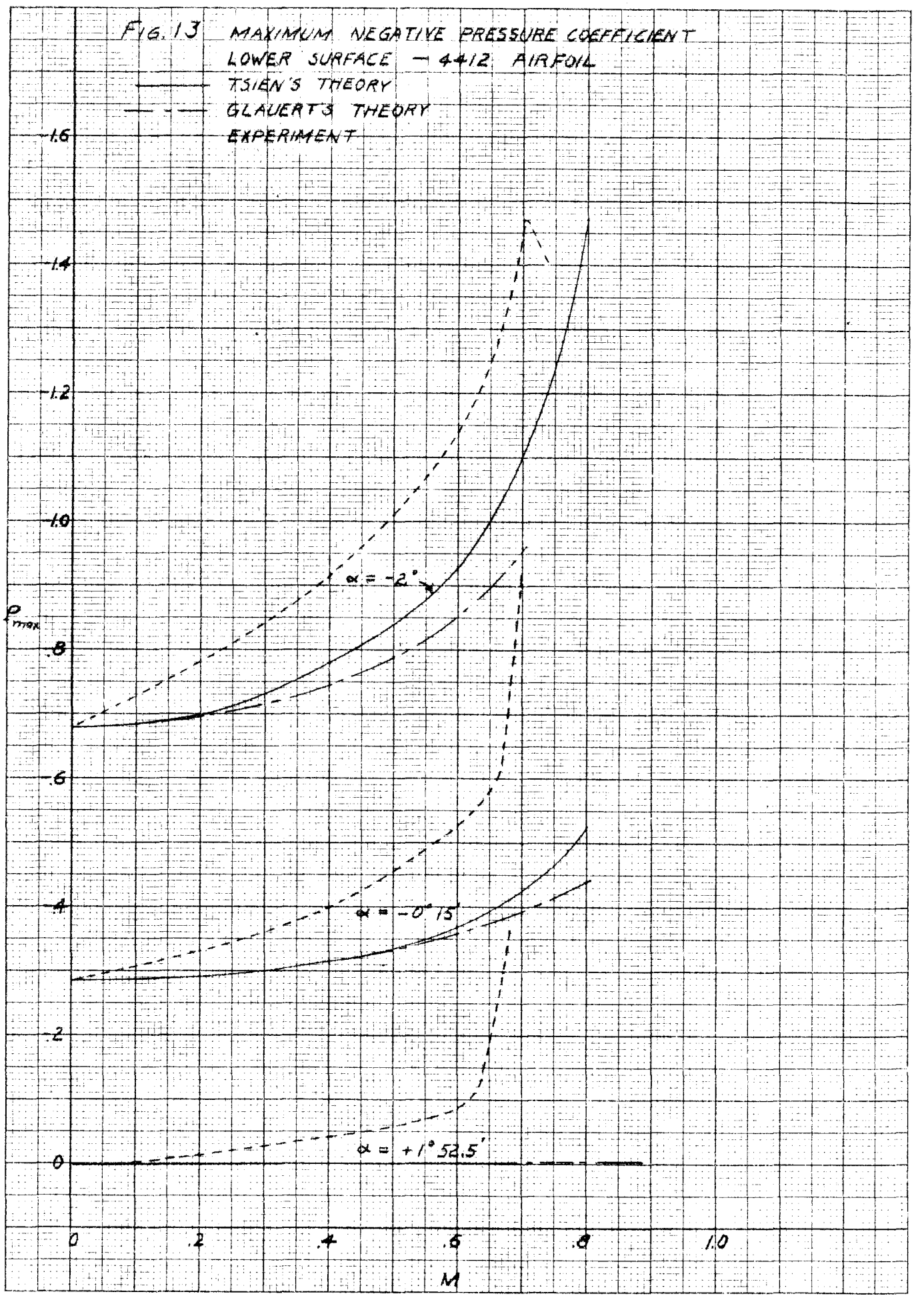
FIG. 13 MAXIMUM NEGATIVE PRESSURE COEFFICIENT
LOWER SURFACE — 4412 AIRFOIL
TSIEN'S THEORY
GLAUERT'S THEORY
EXPERIMENT
-1.6
-1.4
-1.2
-1.0
-.8
-.6
-.4
-.2
0
P_{max}
$\alpha = -2°$
$\alpha = -0° 15'$
$\alpha = +1° 52.5'$
0
.2
.4
.6
.8
1.0
M

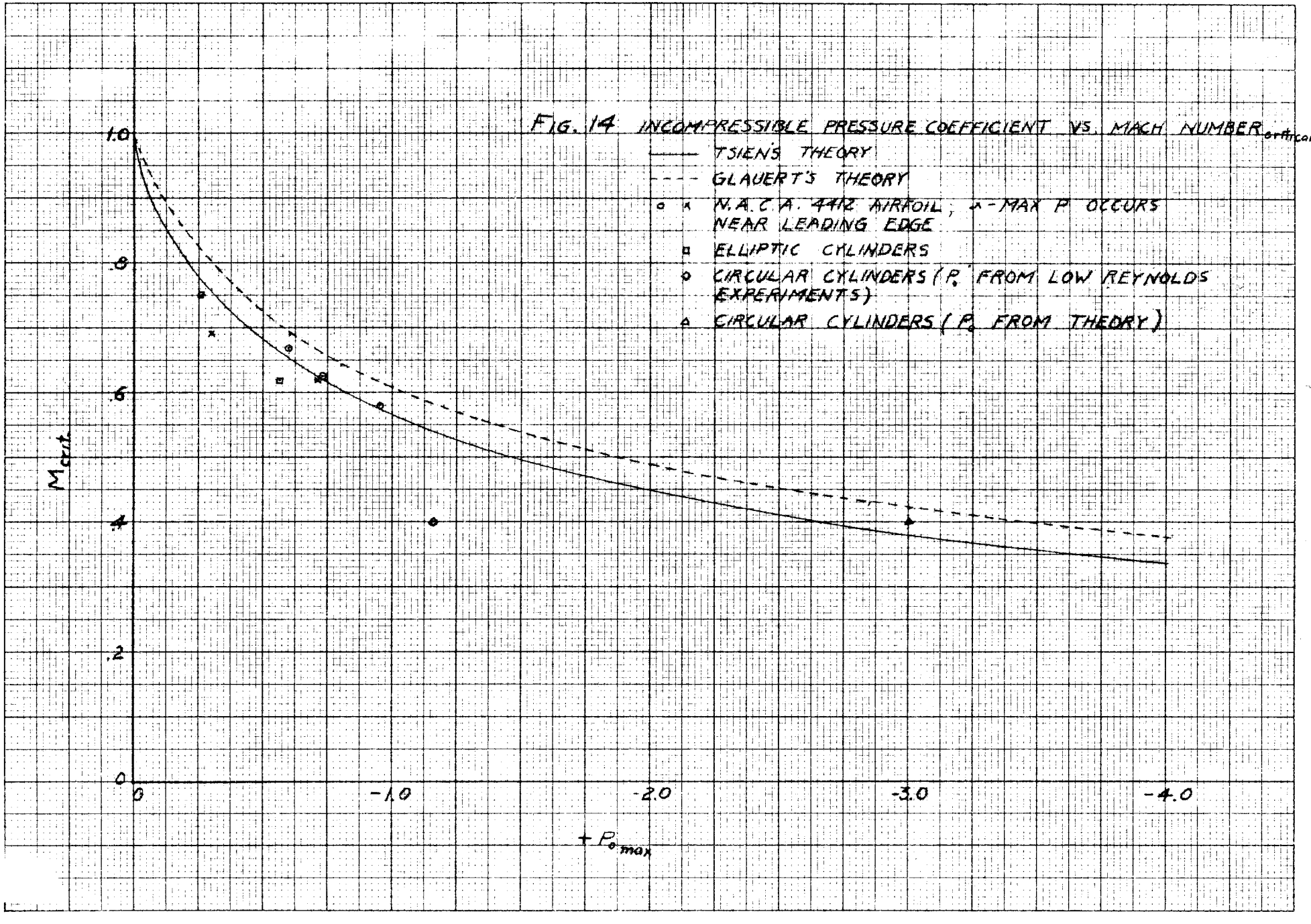
FIG. 14 INCOMPRESSIBLE PRESSURE COEFFICIENT VS. MACH NUMBER critical
TSIEN'S THEORY
GLAUERT'S THEORY
N.A.C.A. 44I2 AIRFOIL, ↑ - MAX P OCCURS NEAR LEADING EDGE
ELLIPTIC CYLINDERS
CIRCULAR CYLINDERS (P_o FROM LOW REYNOLDS EXPERIMENTS)
CIRCULAR CYLINDERS (P_o FROM THEORY)
$M_{crit.}$
1.0
.8
.6
.4
.2
0
0
-1.0
-2.0
-3.0
-4.0
$+P_{o\,max}$

Sta.	U'pr	L'w'r
0	0	0
1.25	2.44	-1.43
2.5	3.39	-1.95
5.0	4.73	-2.49
7.5	5.76	-2.74
10	6.59	-2.74
15	7.89	-2.88
20	8.80	-2.74
25	9.41	-2.50
30	9.76	-2.26
40	9.80	-1.80
50	9.19	-1.40
60	8.14	-1.00
70	6.69	- .65
80	4.89	- .39
90	2.71	- .22
95	1.47	- .16
100	0	0

L. E. Rad.: 1.58
Slope of radius through end of chord: 4:20

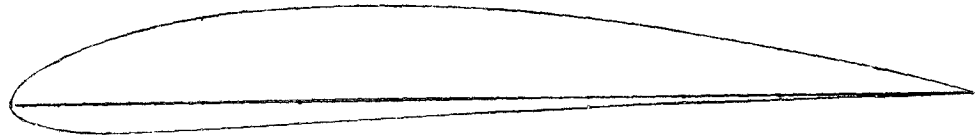

Fig. 15. The 4412 airfoil

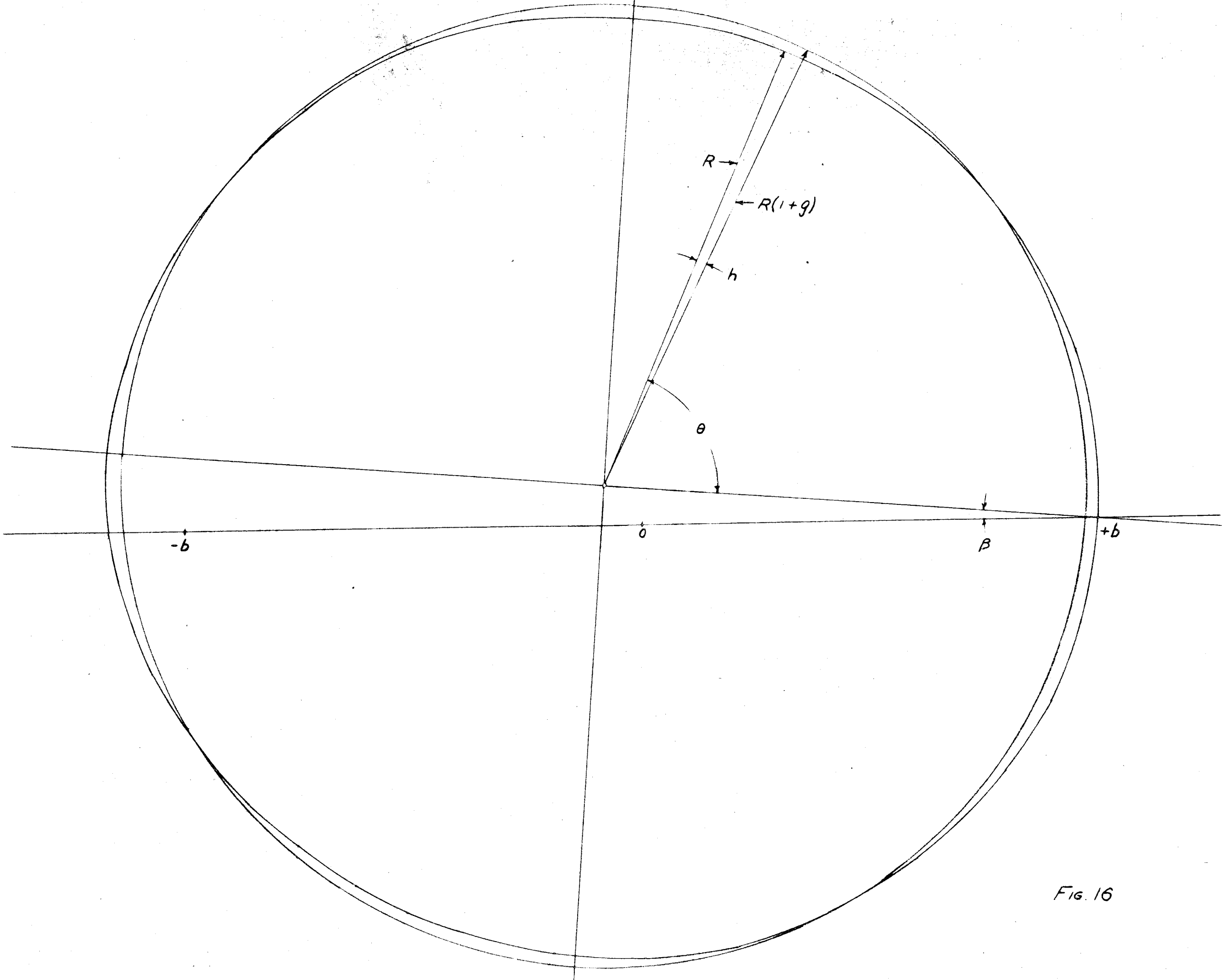

FIG. 16

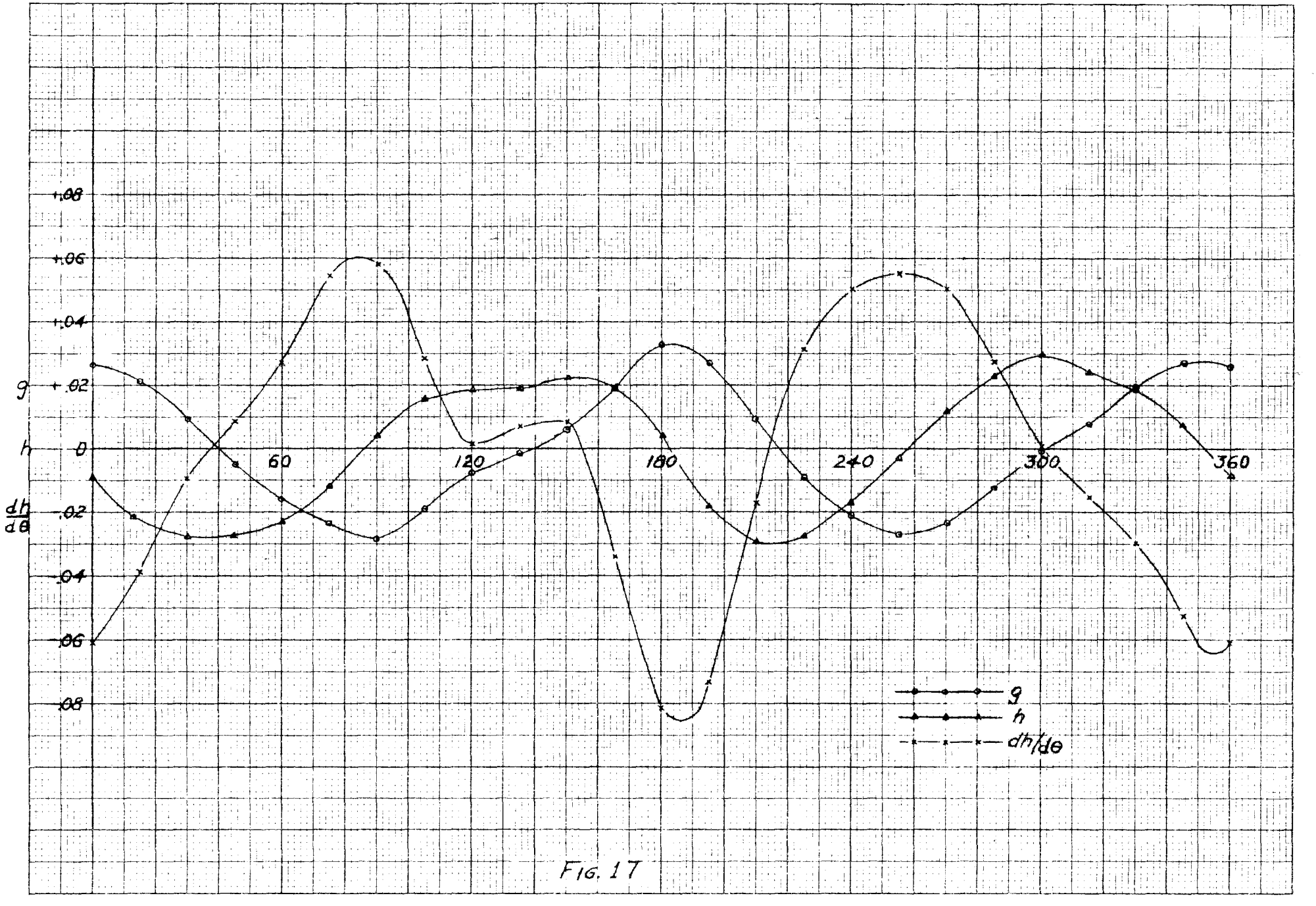

FIG. 17